Theor Chem Acc (2010) 127:419–427
DOI 10.1007/s00214-010-0730-x

REGULAR ARTICLE

Theoretical study on dithieno[3,2-*b*:2′,3′-*d*]phosphole derivatives: high-efficiency blue-emitting materials with ambipolar semiconductor behavior

Jie Wu · Shuixing Wu · Yun Geng · Guochun Yang · Shabbir Muhammad · Junling Jin · Yi Liao · Zhongmin Su

Received: 1 December 2009 / Accepted: 26 January 2010 / Published online: 14 February 2010
© Springer-Verlag 2010

Abstract Phosphole-based systems due to the unique electronic and optical properties have recently been paid much attention as optoelectronic materials. In this work, the relationship among the electronic structure, charge injection, and transport was investigated for five derivatives of dithieno[3,2-*b*:2′,3′-*d*]phosphole (systems **1**–**5**). The structures of systems **1**–**5** in the ground (S_0) and the lowest singlet excited (S_1) states were optimized at the HF/6-31G* and CIS/6-31G* levels of theory, respectively. Based on these structures, electronic spectra were calculated by time-dependent density functional theory. The simulated emission peaks of five phosphole derivatives locating at the blue–green region (448–516 nm), are in good agreement with the experimental data. Compared with tris-(8-quinolinolate) aluminum (III) (Alq_3), normally used as an excellent electron transporter, systems **1**–**5** show a significant improvement in electron affinity (EA) due to σ^*–π^* hyperconjugation, which can effectively promote ability of electron injection**.** The small differences between λ_h and λ_e for systems **1**–**5** (0.06–0.14 eV) facilitate charge transfer balance, which suggests systems **1**–**5** can act as potential ambipolar materials. Owing to good rigidity, low-lying LUMO levels, delocalized frontier molecular orbitals, and the small reorganization energies, the five derivatives of dithieno[3,2-*b*:2′,3′-*d*]phosphole are expected to be high-efficiency blue materials in single-layer OLEDs.

Keywords Phosphole · Electron spectrum · σ^*–π^* Hyperconjugation · Electron injection · Reorganization energy · Density functional theory

1 Introduction

The use of organic semiconducting materials for applications in optoelectronic devices such as field effect transistors (FETs) [1–5], organic light emitting diodes (OLEDs) [6–11], photovoltaics (PVs) [12–14], and sensors [15, 16] has brought forth plenty of remarkable discoveries and continues to hold the limelight in scientific community. OLEDs are currently the subject of an intense research effort due to their promise as devices for full-color display applications [7, 10, 14, 17, 18]. The three primary colors (red, green, and blue) are needed to achieve full-color flat-panel display. While red and green emitters for OLEDs have become readily available by now, efficient and stable organic blue emitters are still rare, since the larger band gap energy of the emission material often inhibits the injection of carriers [18–20]. This has limited the development of the blue electroluminescent materials to some extent, thus constraining the development of organic full-color displays. Furthermore, the performance of OLEDs also depends on charge injection and transport, and charge carrier balance. Highly fluorescent or phosphorescent organic materials of interest in OLEDs tend to have either hole transport (*P*-type) or electron transport (*N*-type) characteristics [9, 10, 21]. However, very often *P*-type

Electronic supplementary material The online version of this article (doi:10.1007/s00214-010-0730-x) contains supplementary material, which is available to authorized users.

J. Wu · S. Wu · Y. Geng · G. Yang · S. Muhammad · J. Jin · Z. Su (✉)
Institute of Functional Material Chemistry, Faculty of Chemistry, Northeast Normal University, Changchun, Jilin 130024, People's Republic of China
e-mail: zmsu@nenu.edu.cn

Y. Liao
College of Chemistry, Capital Normal University, Beijing 100048, People's Republic of China

behavior has been found to be dominating. Scarce of materials with both *P*-type and *N*-type (ambipolar) behaviors leading to charge transfer imbalance severely influences the development of OLEDs in a certain extent [9, 22]. It is vital time to develop and study high-efficiency blue materials with ambipolar semiconductor behavior.

For decades, among the wide range of charge transporting materials reported in the literature, π-conjugated oligomers and polymers based on heteropentacenes containing pyrrole, thiophene, and silole have been widely exploited and used [5, 6, 23, 24] in optoelectronic devices. Phospholes, described in 1959 for the first time [25], are now regarded as promising frameworks for the construction of new classes of π-conjugated organic materials. Phosphole-based systems have recently been paid much attention as optoelectronic materials due to the presence of low-lying lowest unoccupied molecular orbital (LUMO), easy accessibility, and tunableness by chemical modifications at phosphorus center [17, 26–32]. Réau and Baumgartner et al. had put in a lot of efforts in enhancing electronic and optical properties via extending π-conjugated framework over five ring and modifying simply at either the phosphorus center by oxidation (E = O, S), complexation with main group centers (E = BH_3, CH_3^+) or transition metals (E = AuCl), or by variation of the substitution pattern (R on the central phosphorus atom) [27–35].

Understanding the relationship between molecular structure and optical properties of materials is a key point for providing guideline for device design, and a great theoretical research effort is currently being made in this regard [36–43]. However, few blue materials with ambipolar semiconductor behavior have been designed in theory. In this paper we thoroughly investigate the electronic structure of phosphole and systematically report a study of five dithieno[3,2-*b*:2′,3′-*d*]phosphole derivatives, i.e., system **1** (E = lone pair), **2** (E = S), **3** (E = S), **4** (E = AuCl), and **5** (E = BH_3) as theoretically studied chemical models (see Fig. 3). We selected this kind of compounds based on that (1) their experimental emission λ_{max} is concentrated at the blue–green region (440–483 nm) [34],and (2) it has previously been reported that systems **1**–**5** may be excellent candidates for ambipolar semiconductors due to low-lying LUMO levels. The purpose of present work is to investigate the relationship among the electronic structure, electronic spectra, charge injection and transport, and hopefully lay a foundation for designing new ideal high-efficiency blue materials with ambipolar semiconductor behavior.

2 Computational details

All calculations on these phospholes under investigation in this work have been performed using Gaussian 03 program package [44]. The structures of five phosphole derivatives in the ground (S_0) and the lowest singlet excited (S_1) states were optimized at the HF/6-31G* and CIS/6-31G* level of theory, respectively. Based on the ground and excited state structures, absorption and emission spectra were calculated by time-dependent density functional theory (TD-DFT). Fragment orbital correlation has been analyzed by using AOMix.

In the ionization energy (IP) and electron affinity (EA) calculation, the geometric structures of neutral and ions were obtained with B3LYP/6-31G* method. IP can be defined as the variations of energy extracting an electron from a chemical system. EA can be viewed as the variations of energy adding an electron to a chemical system [45, 46]. They are used for evaluating charge injection and transport properties in OLEDs. The charge transport rate (k) is a determining factor for the development of new organic optoelectronic materials and devices. There are two widely used theories for treating carrier motion in organic material, namely the band theory [47, 48] and hopping model [49–55]. The hopping model is suitable for our case, because the intermolecular interactions are weak for the most thin-film amorphous materials in OLEDs [42]. The charge transport mechanism can be described as a self-exchange transfer process, in which an electron or hole transfer occurs from one charged molecule to an adjacent neutral molecule. It can be described as$M^- + M = M + M^-$. According to the semiclassical Marcus theory [56, 57], the electron-transfer rate, k_{ET}, can be described to a good approximation as

$$k_{\mathrm{ET}} = \frac{4\pi^2}{h}\frac{1}{\sqrt{4\pi\lambda k_{\mathrm{B}}T}}V^2 \exp\left\{-\frac{\lambda}{4k_{\mathrm{B}}T}\right\} \quad (1)$$

where λ is the reorganization energy, V is the electronic coupling element (transfer integral) between neighboring molecules, h is Planck's constant, k_B is the Boltzmann constant, and T is the temperature. The two key parameters that dominate the electron-transfer rate are the reorganization energy (λ) and the electronic coupling element (V). The λ and V values must be minimized and maximized, respectively, to ensure high the electron-transfer rate. In this work, we mainly investigate the influence of different substituents on electronic and optical properties of single molecule, thus preliminary predicted charge transport properties by effect of the λ on carriers transfer rates. The λ is the sum of two energetic terms: the intramolecular reorganization energy of the molecule (the inner λ) and the reorganization energy of surrounding medium (the outer λ). The latter is due to the electronic and nuclear polarization of the surrounding medium. In solution, solvent reorganization (the outer λ) is often the dominant contributor [58–60] and affected by the solvent with different dielectric constant [61]. For most practical

purposes, organic electronic materials can be considered to be solid-state systems in which the phonon-like modes of environment are sufficiently stiff and the medium contribution to the relaxation energy ought to be small [62–64]. As to the model system discussed here, which is used as organic electronic materials in the optoelectronic devices, only the inner reorganization energy has been explicitly considered. Furthermore, considering the fact that λ value strongly depends on the theoretical method chosen [65–67], we tested the conventional DFT-based methods with different exchange–correlation functional and confirmed that the B3LYP/6-31G* level is reliable to calculate the intramolecular reorganization energy for predicting charge transport properties in our adopted systems. The intramolecular reorganization energy can be expressed as and be calculated as following Fig. 1 and Eq. 2:

$$\lambda_e = \lambda_0 + \lambda_- = [E^-(M) - E^-(M^-)] + [E(M^-) - E(M)] = EEP - EA_V \quad (2)$$

where $E(M)$ and $E^-(M)$ represent the energy of the neutral and anion with the geometry of the neutral; while $E(M^-)$ and $E^-(M^-)$ represent the energy of the neutral and anion with the geometry of the anion. *EEP* represents the energy difference between the neutral and anion with the geometry of the anion.

3 Results and discussion

3.1 Electronic structure of phosphole

Heretofore, phospholes are the most investigated *P*-derivatives for the design of π-conjugated materials due to their unique electronic and optical properties. Compared with planar pyrrole and thiophene, the orbital interaction of the phosphorus lone pair with the conjugated system for phosphole is inhibited because of the pyramidal environment of the tricoordinated phosphorus center [34]. Calculations at B3LYP/6-31G* level of theory have shown that the LUMO level of phosphole is lowest in energy but the highest occupied molecular orbital (HOMO) levels are close to each other in three heterocyclopentadienes (see Fig. 2). Phosphole has a lobe on phosphorus in-phase with lobes on the adjacent ring carbons in the LUMO, while pyrrole and thiophene have no such a lobe on carbon but a butadiene-like LUMO only. The difference in their LUMO levels is due to the peculiar orbital interaction in the phosphole ring, as shown in Fig. 3. The molecular orbital for phosphole is illustrated by the orbital interaction of a butadiene moiety and a methylphosphine moiety. It is obviously seen that the low-lying LUMO (−0.97 eV) in phosphole mainly originates from interaction between the π^* orbital of the butadiene moiety and the σ^* orbital of the exocyclic P–C bond, i.e., σ^*–π^* hyperconjugation, whereas the LUMO in pyrrole no such interaction. The similar situation of the lowered LUMO level induced by the σ^*–π^* hyperconjugation in silole, clearly illustrated in 1996 [68], has been successfully introduced to explain the unique electronic properties of silole-based systems [69–71]. This sets the stage for the following study of five dithieno[3,2-b:2′,3′-d]phosphole derivatives, and constructing new σ- and π-conjugated systems having low-lying LUMO level in future work.

3.2 Geometry structure and electronic spectra

The geometrical structures of five derivatives of dithieno[3,2-*b*:2′,3′-*d*]phosphole (systems **1**–**5**) and relative systems were optimized without symmetry constraints by

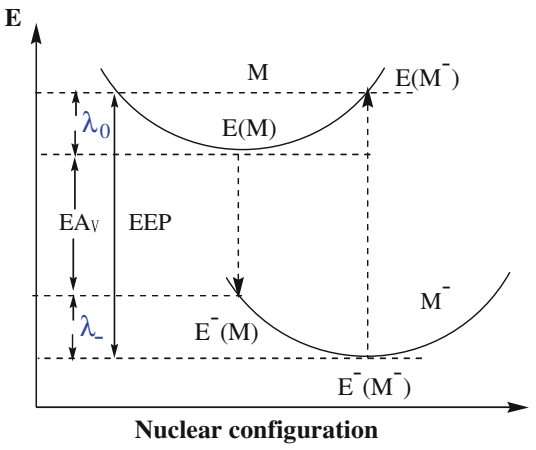

Fig. 1 Sketch of the potential energy surfaces for neutral and anion, showing the vertical transitions (*dash lines*), and the neutral (λ_0) and anion (λ_-) relaxation energies

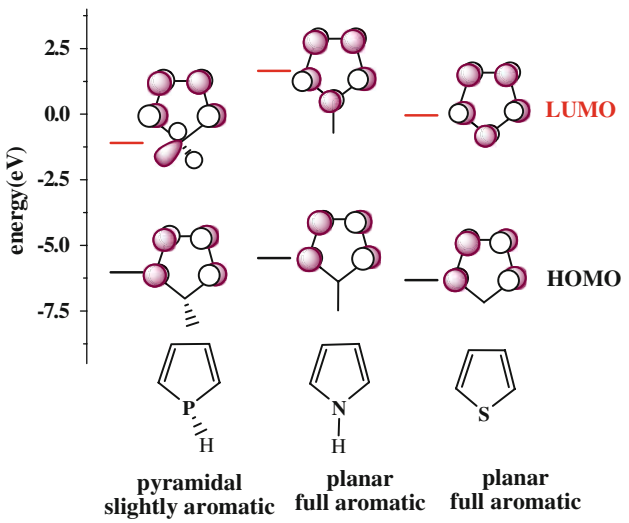

Fig. 2 The HOMOs and LUMOs (B3LYP/6-31G*) for three heterocyclopentadienes

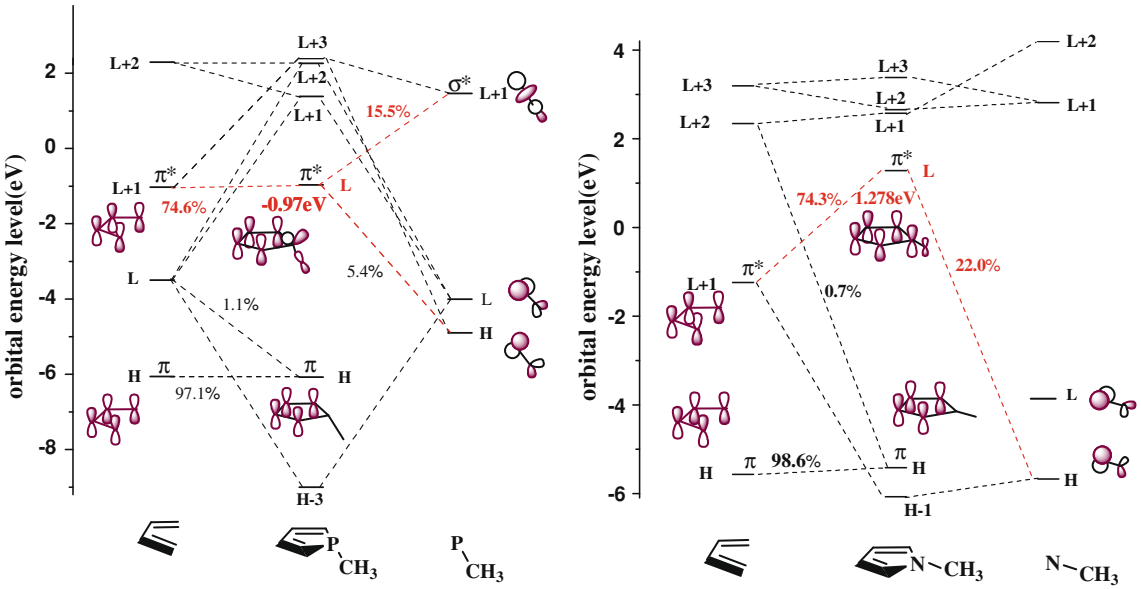

Fig. 3 Molecular orbital correlation diagram for phosphole and pyrrole, calculated at B3LYP/6-31G* level of theory

Fig. 4 Geometric structures of systems **1**–**5** and reference system DBT

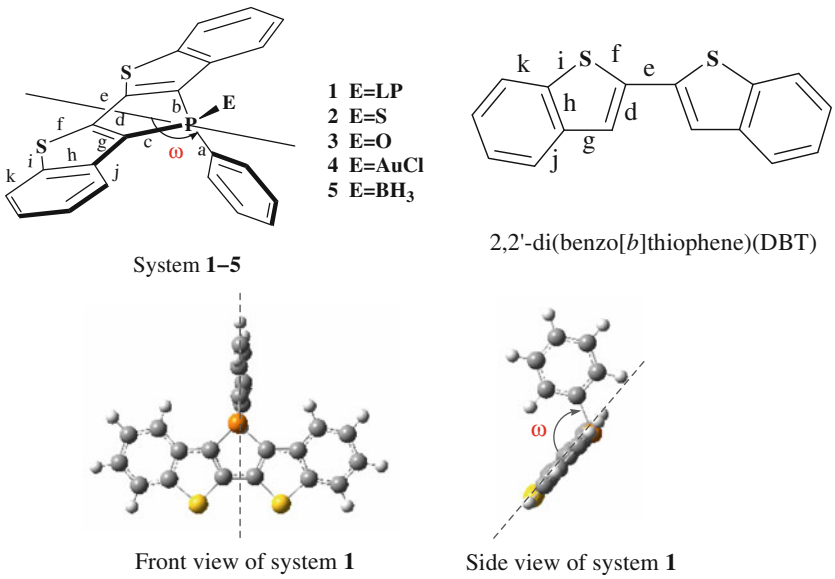

HF/6-31G* level of theory. Systems **1**–**5** all have a Cs symmetry with phenyl ring as the symmetry plane which bisects CPC angle of dithienophosphole moiety (see front view) in Fig. 4. The geometrical structures of systems **1**–**5** in the ground (S_0) (HF/6-31G*) and the lowest singlet excited (S_1) (CIS/6-31G*) states are listed in Table 1. Among them, the folding angle ω is defined as an angle between the mean plane of dithienophosphole moiety and the P–C bond (see side view) Fig. 5.

It can be seen from Table 1 that the introduction of four kinds of substituents at *P*-position has a certain effect on the folding angle and the phosphole ring moiety, whereas having little effect on the remote benzothiophene ring fragment outside the phosphole ring moiety. To evaluate the relaxation of bond length upon substitution as a whole, we employ the concept of the difference between the average length of the "single" and "double" bonds. The degree of bond length alternation (BLA) has been used as a structural parameter in interpreting electronic spectra of many classes of conjugated molecules [38, 72, 73], strongly depending on the theoretical method chosen. In this paper, BLA is defined as follows:

Table 1 Selected bond lengths (Å) the folding angles (ω) (deg) and bond length alternation (BLA) (Å) at optimized ground states with HF/6-31G* compared with the lowest excited states optimized with CIS/6-31G*

Structural parameter	**1** [$S_0/S_1(\Delta)$]	**2** [$S_0/S_1(\Delta)$]	**3** [$S_0/S_1(\Delta)$]	**4** [$S_0/S_1(\Delta)$]	**5** [$S_0/S_1(\Delta)$]	DBT [$S_0/S_1(\Delta)$]
a	1.842/1.860 (0.018)	1.826/1.833 (0.007)	1.814/1.820 (0.006)	1.824/1.838 (0.014)	1.824/1.839 (0.015)	–
b	1.830/1.823 (−0.007)	1.819/1.797 (−0.022)	1.820/1.797 (−0.023)	1.815/1.799 (−0.016)	1.818/1.804 (−0.014)	–
c	1.830/1.823 (−0.007)	1.819/1.797 (−0.022)	1.820/1.797 (−0.023)	1.815/1.799 (−0.016)	1.818/1.804 (−0.014)	–
d	1.350/1.430 (0.080)	1.346/1.430 (0.084)	1.346/1.430 (0.084)	1.350/1.431 (0.081)	1.348/1.431 (0.083)	1.343/1.411 (0.068)
e	1.453/1.371(−0.082)	1.464/1.375 (−0.089)	1.468/1.377 (−0.091)	1.460/1.374 (−0.086)	1.460/1.373 (−0.087)	1.463/1.385 (−0.078)
f	1.741/1.748 (0.007)	1.734/1.743 (0.009)	1.734/1.742 (0.008)	1.733/1.742 (0.009)	1.735/1.744 (0.009)	1.759/1.775 (0.016)
g	1.446/1.411 (−0.035)	1.443/1.414 (−0.029)	1.443/1.415 (−0.028)	1.444/1.412 (−0.032)	1.440/1.411 (−0.029)	1.445/1.394 (−0.051)
h	1.400/1.416 (0.016)	1.399/1.413 (0.014)	1.400/1.413 (0.013)	1.400/1.415 (0.015)	1.400/1.415 (0.016)	1.395/1.423 (0.028)
i	1.758/1.771 (0.013)	1.758/1.770 (0.012)	1.758/1.770 (0.012)	1.758/1.770 (0.012)	1.758/1.778 (0.020)	1.748/1.752 (0.004)
j	1.398/1.409 (0.011)	1.398/1.407 (0.009)	1.398/1.407 (0.009)	1.398/1.408 (0.010)	1.398/1.409 (0.011)	1.398/1.422 (0.024)
k	1.390/1.379 (−0.011)	1.390/1.380 (−0.010)	1.390/1.381 (−0.009)	1.390/1.380 (−0.010)	1.390/1.380 (−0.010)	1.391/1.382 (−0.009)
BLA	0.099/0.168 (0.069)	0.095/0.163 (0.068)	0.093/0.161 (0.068)	0.096/0.164 (0.068)	0.098/0.167 (0.069)	0.096/0.170 (0.074)
ω (deg)	114.09/109.59 (−5.50)	114.98/117.51 (2.53)	115.13/118.83 (3.70)	117.43/115.03 (−2.40)	116.64/113.87 (−2.77)	–

$$\mathrm{BLA} = \frac{d+f+i+h+j}{5} - \frac{e+g+k}{3} \quad (3)$$

To accurately estimate the BLA values, we tested different methods with the 6–31G* basis set (see Supporting information). As shown in Fig. S1, the BLA value at the BHandHLYP level (marked with pink) perfectly matches the experiment value. Note that the trend of BLA in (from left to right) systems **1**–**5** by the HF method is well in agreement with that by BHandHLYP (Fig. S1). So HF method is also reliable to be employed to investigate the influence of different substituents on the BLA value in the work. The results at the HF/6–31G* level show the similar BLA values of systems **1**–**5** in the ground state (S_0) (0.093–0.099 Å) and the nearly constant ΔBLA values from S_0 to S_1 states (CIS/6–31G*) for systems **1**–**5** (0.068–0.069 Å). This suggests the introduction of substituents has little effect on geometry backbone of systems **1**–**5**. In addition, ΔBLA of systems **1**–**5** are relatively smaller than that of 2, 2′-di(benzo[*b*]thiophene)(DBT) (0.074 Å), which indicates that the phosphinidyne has a certain restriction in structural relaxation and these systems have excellent rigidity, which may lead to a significant improvement in emission efficiency.

Based on the structural analysis of systems **1**–**5**, the absorption and emission spectra were calculated at S_0 and S_1 geometries using TD-DFT method to study their optical properties. The wavelengths for absorption and emission (λ_{max}), oscillator strengths, main transition contribution, and experimental data have been listed in Table 2. The main absorption and emission peaks all arise from the promotion of one electron between S_0 and S_1. The lowest $S_0 \rightarrow S_1$ electronic transitions for them originate from HOMO → LUMO transition, i.e., $\pi \rightarrow \pi^*$ transition, by reason that the HOMOs are all π bonding orbitals while the LUMOs are π^* antibonding orbitals. This indicates introducing different substituents at *P*-position does not affect main transition character of absorption and emission spectra. However, different substituents have great influence on the oscillator strengths. For example, the oscillator strength of system **1** is largest among them. The oscillator strength for an electronic transition is proportional to the transition moment. In turn, the transition moment reflects the transition probability between S_0 and S_1. Thus, system **1** may have more intense emission. Moreover, the emission peaks of systems **1**–**5** are concentrated approximately at the blue-green ray region (448–516 nm). Although the experimental emission wavelengths were not predicted exactly, the general trend of emission wavelengths (**1** > **5** > **4** > **2** > **3**) was captured by our calculation. This may lay a theoretical basis for the future to design high-performance pure-blue emission material.

From the electronic spectrum analysis (see Table 2), all of the S_1 transitions are characterized by electron

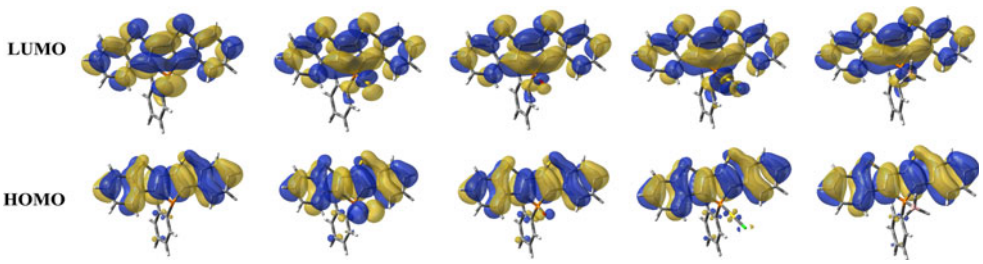

Fig. 5 Frontier molecular orbital diagrams by B3LYP/6-31G* calculation

Table 2 Absorption and emission energies (nm), main transition contribution and oscillator strengths (*f*) at the TDDFT B3LYP/6-31G* level compared with experimental Data

Molecule	Absorption spectra			Emission spectra		
	λ/nm (*f*)	Main transition	Exp.[a]	λ/nm (f)	Main transition	Exp.[a]
1	357 (0.47)	H → L	385	448 (0.36)	H → L	440
2	390 (0.26)	H → L	435	508 (0.17)	H → L	473
3	387 (0.33)	H → L	424	516 (0.25)	H → L	483
4	390 (0.28)	H → L	398	498 (0.24)	H → L	471
5	368 (0.41)	H → L	407	469 (0.32)	H → L	461

[a] Measured in CH_2Cl_2 [34]

promotion from the HOMO to the LUMO. So the relaxation of the structures between S_0 and S_1 can also be determined from the character of the frontier molecule orbital involved in the excited transition. The HOMO is bonding across the *d*, *h*, *i*, and *j* bonds, whereas the LUMO has a node plane in the regions. On the contrary, the HOMO has nodes across the *e* and *g* bonds, but the LUMO is bonding. According to molecular orbital (MO) nodal patterns theory [74], one would expect that *d*, *h*, *i*, and *j* bonds are lengthened, whereas the *e* and *g* bonds are shortened from S_0 to S_1. The data in Table 1 just confirm the anticipated changes of these bonds. Furthermore, the distribution of frontier molecular orbital in systems **1**–**5** is basically similar and the HOMO and LUMO are evenly delocalized throughout the conjugated fragments. These features are favorable to transport both hole and electron.

3.3 Electron injection and transport properties

A good device performance of OLED is attributed to charge injection, transport, and the comparable balance between the holes and electrons [9, 24]. The ionization potential (IP) and the electron affinity (EA) are usually main factors in evaluating the efficiency of charge injection in different OLED materials. EA or reduction potential and IP or oxidation potential corresponds to the LUMO and HOMO energy levels of a molecule, respectively [24]. In experiment, the LUMO energy level is usually estimated from the ionization potential and the optical band gap. In theory, we can directly figure out EA or LUMO energy level and IP or HOMO energy level which can be used to evaluate abilities of charge injection. Figure 6 is a schematic diagram of a single-layer OLED. It is well known that the larger EA value of material, the easier an electron from the cathode will cross the barrier (ΔE_e) for electron injection from the electrode such as the Al and Ca. Likewise, the smaller IP value of material, the easier a hole transfers from the anode (ITO) to the adjacent hole transport layer in OLEDs. Compared with Alq_3 ($EA_v = 0.83$ eV at B3LYP/6-31G* level) [75], which is well-known as an excellent electron transporter [10, 76, 77], systems **2**–**5** show a significant improvement in EA, which can effectively promote ability of electron injection. It is noteworthy that systems **2**–**5** exhibit considerably lower LUMO energy levels, a decrease of about 0.4–0.8 eV versus that of system **1**, suggesting that

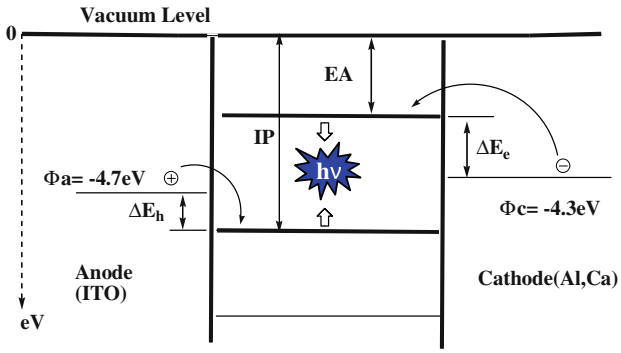

Fig. 6 Energy-level diagrams of a single-layer OLED

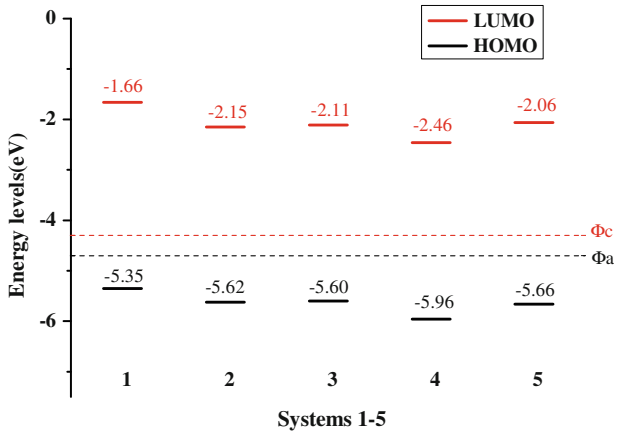

Fig. 7 Relative HOMO and LUMO energy level for systems **1**–**5** by B3LYP/6-31G* calculation, and work function of ITO and Al, Ca

introducing different substituents at *P*-position remarkably affects the LUMO energy levels Fig. 7.

For more in-depth analysis of the influence of different substituents at *P*-position on the σ^*–π^* conjugation, we carried out fragment orbital calculations for system **4** with lowest LUMO level (−2.46 eV) and system **1** (−1.69 eV) at the B3LYP/6-31G* level. We divided systems **1** and **4** into fragment I possessing the endocyclic π system and fragment II having the exocyclic P–C bond (see Fig. 8). The results show system **4** (E = AuCl) has a much lower-lying LUMO by about 0.77 eV and a little lower-lying HOMO by about 0.63 eV than system **1** (E = LP). This can be rationalized by the fact that the LUMOs of systems **1** and **4** arise from mixture of the σ^* orbital of fragment II with the π^* orbital of fragment I, while the HOMOs of systems **1** and **4** almost come from the HOMOs of fragment **I**. Additionally, σ^* orbital level of fragment II in system **4** (−0.2 eV) is much lower than that in system **1** (1.21 eV), whereas π^* orbital level (−1.70 eV) of fragment I in system **4** is close to that (−1.75 eV) in system **1**. This suggests the introduction of −AuCl group at *P*-position enhances the σ^*–π^* hyperconjugation and further lowers LUMO level of the complex, with the effect on the σ^* orbital level of fragment II being much more pronounced than that on π^* orbital level. Our calculations may lay a theoretical foundation for constructing new σ and π-conjugated materials having low-lying LUMO level.

Reorganization energy (λ) is generally used as the main aspect to assess the charge transport rate. In λ calculations, considering the fact that λ value strongly depends on the theoretical method chosen [63–65], we tested the conventional DFT-based methods with different exchange–correlation functional on systems **1**–**3**. The results show a general trend exists that the more the percentage of HF exchange in different DFT-based methods, the larger the $\lambda_{h/e}$ values are (Fig. S3 of Supporting information). It is worth noting that the differences between λ_h and λ_e ($\Delta\lambda_{h/e}$) for each system with different DFT-based methods are similar. For example, different DFT-based methods give $\Delta\lambda_{h/e}$ = 0.05–0.06, 0.11–0.14, 0.11–0.14 eV for systems **1**–**3**, respectively (Table S2). This shows that selecting different DFT-based methods has little influence on the final conclusion that systems **1**–**3** can act as potential ambipolar materials. Thus, the B3LYP hybrid density functional can be used as a reliable method to calculate inner reorganization energies in our adopted systems. In the case, the λ_h and λ_e for systems **4**–**5** were calculated with the B3LYP functional and the 6–31G* basis set (Table 3). Similarly, although the λ_e for systems **4**–**5** (0.38 eV) are slightly larger than λ_h for them (0.29–0.31 eV), the differences between λ_h and λ_e for them (0.07–0.09 eV) are

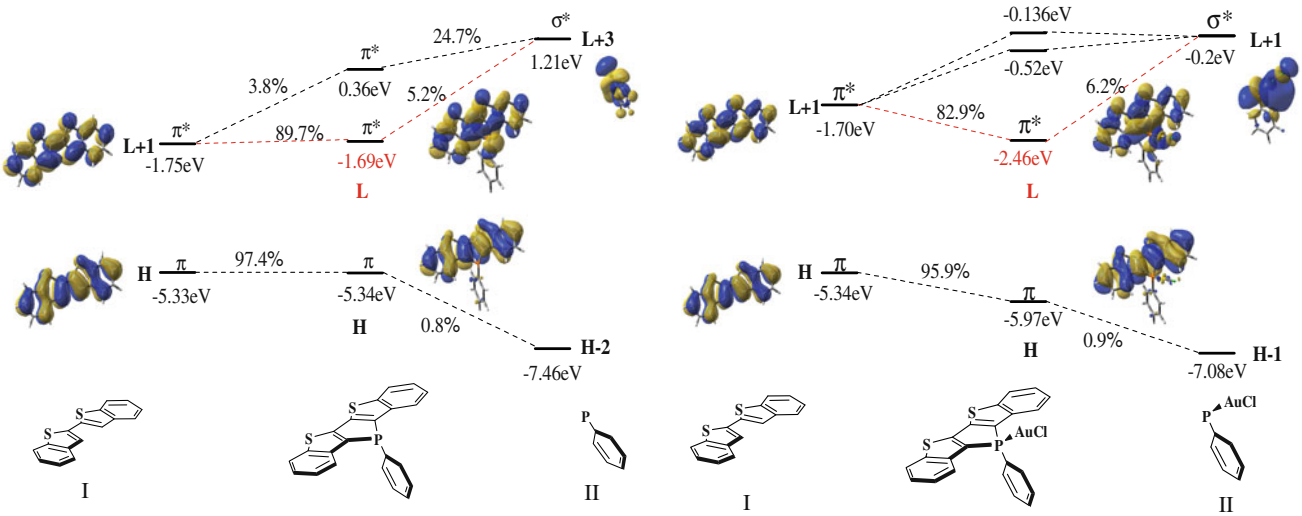

Fig. 8 Orbital interaction diagram for systems **1** and **4** which is formed by two fragments (IandII) at the B3LYP/6-31G* level of theory

Table 3 HOMO-LUMO gap, vertical ionization potential (IP_v), vertical electron affinity (EA_v), extraction potential and intramolecular reorganization energy ($\lambda_{h/e}$) by B3LYP/6-31G* calculation (All units in eV)

Molecules	Δ_{H-L}	IP_v	EA_v	HEP	EEP	λ_h	λ_e
1	3.69	6.67	0.35	6.40	0.68	0.27	0.33
2	3.47	6.91	0.84	6.64	1.25	0.27	0.41
3	3.49	6.93	0.77	6.63	1.18	0.30	0.40
4	3.50	7.26	1.20	6.95	1.58	0.31	0.38
5	3.60	6.97	0.75	6.68	1.13	0.29	0.38

small, which facilitates charge transfer balance and the formation of the exciton. Thus, systems **1–5** can act as high-efficiency emitting materials with ambipolar semiconductor behavior.

4 Conclusions

In this paper, we investigated the influence of different substituents (E = LP, E = O, E = S, E = AuCl, $E = BH_3$) at *P*-position on geometrical and electronic structures as well as corresponding consequences on electron injection, transport properties, and luminescent properties by quantum chemistry methods. The introduction of different substituents at *P*-position (E = LP, E = O, E = S, E = AuCl, $E = BH_3$) has little influence on the geometry framework of dithieno[3,2-b:2′,3′-d]phosphole and the distribution of frontier molecular orbitals for systems **1–5**. Meanwhile it increases the σ^*–π^* hyperconjugation, which leads to low-lying LUMO level, thus enhancing the ability of electron injection by varying degrees. System **4** with the lowest LUMO energy levels may be most favorable for the injection of electron into the electron transport material. Furthermore, the main absorption peaks for systems **1–5** all arise from the promotion of one electron from S_0 to S_1. The $S_0 \rightarrow S_1$ for them is mainly HOMO $\rightarrow$ LUMO ($\pi \rightarrow \pi^*$) transition. However, the influence on oscillator strengths of different substituents is relatively large, which will further effect on the emission efficiency. The emission peaks of systems **1–5** are concentrated approximately at the blue-green ray region (448–516 nm), which means our studied systems may be used as blue-emitting material. Calculated reorganization energies (λ) show that five derivatives of dithieno[3,2-b:2′,3′-d]phosphole can act as high-efficiency emitting materials with ambipolar semiconductor behavior in single-layer OLEDs.

Acknowledgments The authors gratefully acknowledge the financial support from the National Natural Science Foundation of China (Project Nos. 20373009, 20703008, 20903020), the Major State Basic Research Development Program (973 Program—2009CB623605), Chang Jiang Scholars Program (2006), Program for Changjiang Scholars and Innovative Research Team in University (IRT0714), the Training Fund of NENU's Scientific Innovation Project (NENU-STC08005), the Science and Technology Development Project Foundation of Jilin Province (20090146), and the Project-sponsored by SRF for ROCS, SEM.

References

1. Dimitrakopoulos CD, Malenfant PRL (2002) Adv Mater 14:99. doi:10.1002/1521-4095(20020116)14:2<99:AID-ADMA99>3.0.CO;2-9
2. Ebisawa F, Kurokawa T, Nara S (1983) J Appl Phys 54:3255. doi:10.1063/1.332488
3. Horowitz G, Hajlaoui ME (2000) Adv Mater 12:1046. doi:10.1002/1521-4095(20007)12:14<1046:AID-ADMA1046>3.0.CO;2-W
4. Nagamatsu S, Kaneto K, Azumi R, Matsumoto M, Yoshida Y, Yase K (2005) J Phys Chem B 109:9374. doi:10.1021/jp044222l
5. Zaumseil J, Sirringhaus H (2007) Chem Rev 107:1296. doi:10.1021/cr0501543
6. Anthony JE (2006) Chem Rev 106:5028. doi:10.1021/cr050966z
7. D'Andrade BW, Forrest SR (2004) Adv Mater 16:1585. doi:10.1002/adma.200400684
8. Huang F, Shih PI, Shu CF, Chi Y, Jen AKY (2009) Adv Mater 21:361. doi:10.1002/adma.200802179
9. Kulkarni AP, Tonzola CJ, Babel A, Jenekhe SA (2004) Chem Mater 16:4556. doi:10.1021/cm0494731
10. Tang CW, VanSlyke SA (1987) Appl Phys Lett 51:913. doi:10.1063/1.98799
11. Williams EL, Haavisto K, Li J, Jabbour GE (2007) Adv Mater 19:197. doi:10.1002/adma.200602174
12. Gunes S, Neugebauer H, Sariciftci NS (2007) Chem Rev 107:1324. doi:10.1021/cr050149z
13. Peumans P, Yakimov A, Forrest SR (2003) J Appl Phys 93:3693. doi:10.1063/1.1534621
14. Yu MX, Chang LC, Lin CH, Duan JP, Wu FI, Chen IC, Cheng CH (2007) Adv Funct Mater 17:369. doi:10.1002/adfm.200600730
15. McQuade DT, Pullen AE, Swager TM (2000) Chem Rev 100:2537. doi:10.1021/cr9801014
16. Thomas SW, Joly GD, Swager TM (2007) Chem Rev 107:1339. doi:10.1021/cr0501339
17. Fave C, Cho T-Y, Hissler M, Chen C-W, Luh T-Y, Wu C-C, Réau R (2003) J Am Chem Soc 125:9254. doi:10.1021/ja035155w
18. Noda T, Ogawa H, Shirota Y (1999) Adv Mater 11:283
19. Kulkarni AP, Jenekhe SA (2003) Macromolecules 36:5285. doi:10.1021/ma0344700
20. Vak D, Lim B, Lee S-H, Kim D-Y (2005) Org Lett 7:4229. doi:10.1021/ol051661+
21. Bernius MT, Inbasekaran M, O'Brien J, Wu W (2000) Adv Mater 12:1737. doi:10.1002/1521-4095(200012)12:23<1737:AID-ADMA1737>3.0.CO;2-N
22. Antoniadis H, Abkowitz MA, Hsieh BR (1994) Appl Phys Lett 65:2030. doi:10.1063/1.112784
23. Hissler M, Dyer PW, Réau R (2003) Coord Chem Rev 244:1. doi:10.1016/S0010-8545(03)00098-5
24. Shirota Y, Kageyama H (2007) Chem Rev 107:953. doi:10.1021/cr050143+
25. Mathey F (2002) Chem Rev 88:429. doi:10.1021/cr00084a005
26. Crassous J, Réau R (2008) Dalton Trans 6865. doi:10.1039/b810976a

27. Dienes Y, Durben S, Kárpáti T, Neumann T, Englert U, Nyulászi L, Baumgartner T (2007) Chem Eur J 13:7487. doi:10.1002/chem.200700399
28. Fadhel O, Gras M, Lemaitre N, Deborde V, Hissler M, Geffroy B, Réau R (2009) Adv Mater 21:1261. doi:10.1002/adma.200801913
29. Fave C, Hissler M, Karpati T, Rault-Berthelot J, Deborde V, Toupet L, Nyulaszi L, Réau R (2004) J Am Chem Soc 126:6058. doi:10.1021/ja0317067
30. Matano Y, Miyajima T, Fukushima T, Kaji H, Kimura Y, Imahori H (2008) Chem Eur J 14:8102. doi:10.1002/chem.200801017
31. Schaefer W, Schweig A, Mathey F (2002) J Am Chem Soc 98:407. doi:10.1021/ja00418a015
32. Su H-C, Fadhel O, Yang C-J, Cho T-Y, Fave C, Hissler M, Wu C-C, Réau R (2006) J Am Chem Soc 128:983. doi:10.1021/ja0567182
33. Baumgartner T, Réau R (2006) Chem Rev 106:4681. doi:10.1021/cr040179m
34. Dienes Y, Eggenstein M, Kárpáti T, Sutherland Todd C, Nyulászi L, Baumgartner T (2008) Chem Eur J 14:9878. doi:10.1002/chem.200801549
35. Sebastian M, Hissler M, Fave C, Rault-Berthelot J, Odin C, Réau R (2006) Angew Chem Int Ed 45:6152. doi:10.1002/anie.200601844
36. Gao HZ, Qin CS, Zhang HY, Wu SX, Su ZM, Wang Y (2008) J Phys Chem A 112:9097. doi:10.1021/jp804308e
37. Kwon O, Coropceanu V, Gruhn NE, Durivage JC, Laquindanum JG, Katz HE, Cornil J, Bredas JL (2004) J Chem Phys 120:8186. doi:10.1063/1.1689636
38. Liao Y, Shi LL, Feng JK, Yang L, Ren AM (2006) J Theor Comput Chem 5:401. doi:10.1142/S0219633606002349
39. Liu Y-L, Feng J-K, Ren A-M (2007) J Comput Chem 28:2500. doi:10.1002/jcc.20753
40. Sancho-Garcia JC, Horowitz G, Bredas JL, Cornil J (2003) J Chem Phys 119:12563. doi:10.1063/1.1625918
41. Teng YL, Kan YH, Su ZM, Liao Y, Yang SY, Wang RS (2007) Theor Chem Acc 117:1. doi:10.1007/s00214-005-0025-9
42. Yang GC, Liao Y, Su ZM, Zhang HY, Wang Y (2006) J Phys Chem A 110:8758. doi:10.1021/jp061286i
43. Zou LY, Ren AM, Feng JK, Liu YL, Ran XQ, Sun CC (2008) J Phys Chem A 112:12172. doi:10.1021/jp8032462
44. Frisch MJ, Trucks GW, Schlegel HB, Scuseria GE, Robb MA, Cheeseman JR, Montgomery JA Jr, Vreven T, Kudin KN, Burant JC, Millam JM, Iyengar SS, Tomasi J, Barone V, Mennucci B, Cossi M, Scalmani G, Rega N, Petersson GA, Nakatsuji H, Hada M, Ehara M, Toyota K, Fukuda R, Hasegawa J, Ishida M, Nakajima T, Honda Y, Kitao O, Nakai H, Klene M, Li X, Knox JE, Hratchian HP, Cross JB, Adamo C, Jaramillo J, Gomperts R, Stratmann RE, Yazyev O, Austin AJ, Cammi R, Pomelli C, Ochterski JW, Ayala PY, Morokuma K, Voth GA, Salvador P, Dannenberg JJ, Zakrzewski VG, Dapprich S, Daniels AD, Strain MC, Farkas O, Malick DK, Rabuck AD, Raghavachari K, Foresman JB, Ortiz JV, Cui Q, Baboul AG, Clifford S, Cioslowski J, Stefanov BB, Liu G, Liashenko A, Piskorz P, Komaromi I, Martin RL, Fox DJ, Keith T, Al-Laham MA, Peng CY, Nanayakkara A, Challacombe M, Gill PMW, Johnson B, Chen W, Wong MW, Gonzalez C, Pople JA (2004) Gaussian 03, Revision C. 02. Gaussian, Inc, Wallingford
45. Curioni A, Andreoni W (2001) IBM J Res Dev 45:101
46. Curioni A, Boero M, Andreoni W (1998) Chem Phys Lett 294:263. doi:10.1016/S0009-2614(98)00829-X
47. Bredas JL, Calbert JP, da Silva DA, Cornil J (2002) Proc Natl Acad Sci USA 99:5804. doi:10.1073/pnas.092143399
48. Cheng YC, Silbey RJ, da Silva DA, Calbert JP, Cornil J, Bredas JL (2003) J Chem Phys 118:3764. doi:10.1063/1.1539090
49. Li X, Tong J, He F (2000) Chem Phys 260:283. doi:10.1016/S0301-0104(00)00283-4
50. Lin BC, Cheng CP, Lao ZPM (2003) J Phys Chem A 107:5241. doi:10.1021/jp0304529
51. Malagoli M, Brédas JL (2000) Chem Phys Lett 327:13. doi:10.1016/S0009-2614(00)00757-0
52. Marcus RA, Sutin N (1985) Biochim Biophys Acta Bioenerg 811:265. doi:10.1016/0304-4173(85)90014-X
53. Nelsen SF, Blomgren F (2001) J Org Chem 66:6551. doi:10.1021/jo001705m
54. Nelsen SF, Trieber DA, Ismagilov RF, Teki Y (2001) J Am Chem Soc 123:5684. doi:10.1021/ja003436n
55. Sakanoue K, Motoda M, Sugimoto M, Sakaki S (1999) J Phys Chem A 103:5551. doi:10.1021/jp990206q
56. Balzani V, Juris A, Venturi M, Campagna S, Serroni S (1996) Chem Rev 96:759. doi:10.1021/cr941154y
57. Marcus RA (1993) Rev Mod Phys 65:599. doi:10.1103/RevModPhys.65.599
58. LeBard DN, Lilichenko M, Matyushov DV, Berlin YA, Ratner MA (2003) J Phys Chem B 107:14509. doi:10.1021/jp035546x
59. Tavernier HL, Fayer MD (2001) J Chem Phys 114:4552. doi:10.1063/1.1349705
60. Tavernier HL, Kalashnikov MM, Fayer MD (2000) J Chem Phys 113:10191. doi:10.1063/1.1323505
61. Pérez F, Hernández M, Prado-Gotor R, Lopes-Costa T, López-Cornejo P (2005) Chem Phys Lett 407:342. doi:10.1016/j.cplett.2005.03.105
62. Beljonne D, Ye AJ, Shuai Z, Bredas JL (2004) Adv Funct Mater 14:684. doi:10.1002/adfm.200305176
63. Hutchison GR, Ratner MA, Marks TJ (2005) J Am Chem Soc 127:2339. doi:10.1021/ja0461421
64. Norton JE, Bredas JL (2008) J Am Chem Soc 130:12377. doi:10.1021/ja8017797
65. Sancho-Garcia JC, Perez-Jimenez AJ (2008) J Chem Phys 129:024103. doi:10.1063/1.2951991
66. Sancho-Garcia JC, Perez-Jimenez AJ (2009) Phys Chem Chem Phys 11:2741. doi:10.1039/b821748c
67. Sancho-García JC, Pérez-Jiménez AJ (2008) J Phys Chem A 112:10325. doi:10.1021/jp802160b
68. Yamaguchi S, Tamao K (1996) Bull Chem Soc Jpn 69:2327
69. Yamaguchi S, Endo T, Uchida M, Izumizawa T, Furukawa K, Tamao K (2000) Chem Eur J 6:1683. doi:10.1002/(SICI)1521-3765(20000502)6:9<1683:AID-CHEM1683>3.0.CO;2-M
70. Yamaguchi S, Endo T, Uchida M, Izumizawa T, Furukawa K, Tamao K (2001) Chem Lett 30:98. doi:10.1246/cl.2001.98
71. Yamaguchi S, Itami Y, Tamao K (1998) Organometallics 17:4910. doi:10.1021/om980393z
72. Kan YH, Yang GC, Yang SY, Zhang M, Lan YQ, Su ZM (2006) Chem Phys Lett 418:302. doi:10.1016/j.cplett.2005.11.005
73. Shi LL, Li T, Zhao SS, Li H, Su ZM (2009) Theor Chem Acc 124:29. doi:10.1007/s00214-009-0573-5
74. Halls MD, Schlegel HB (2001) Chem Mater 13:2632. doi:10.1021/cm010121d
75. Martin RL, Kress JD, Campbell IH, Smith DL (2000) Phys Rev B 61:15804. doi:10.1103/PhysRevB.61.15804
76. Chen CH, Shi J (1998) Coord Chem Rev 171:161. doi:10.1016/S0010-8545(98)90027-3
77. Wang S (2001) Coord Chem Rev 215:79. doi:10.1016/S0010-8545(00)00403-3